

Near-asymptotic angle dependence of ocean optical radiance

Ammar H. Hakim, Brian D. Piening, and Norman J. McCormick

The approach of ocean optical radiance to an approximate asymptotic dependence with increasing depth in spatially uniform waters is numerically examined for a variety of sea surface illumination conditions.
© 2004 Optical Society of America
OCIS codes: 010.0010, 010.4450, 030.5620, 290.4210, 290.7050.

1. Introduction

In deep, spatially uniform waters the radiance tends with increasing depth to an asymptotic state that is azimuthally independent. An example of this phenomenon in everyday life occurs when the direction of the Sun cannot be discerned because sunlight is transmitted through an optically thick, cloudy atmosphere and the light appears the same in all horizontal directions. For light in ocean water, the physical explanation for this tendency to an azimuthal independence is that, because any fluorescence or bioluminescence is essentially isotropic, the only way that the radiance can have an azimuthal dependence is by means of the azimuthal dependence of the surface illumination. Even though each scattering event is strongly anisotropic in the forward direction, each scattering is symmetric in a plane normal to the initial photon direction. Thus, after many scattering events have occurred, the collided radiation that is still present deep beneath the surface tends to not depend on the angular distribution of the surface illumination, and any uncollided portion attenuates exponentially with optical depth until it is only a small fraction of the total radiance. Furthermore, in the limit that the radiance tends with increasing depth to its asymptotic angular distribution, it is uncoupled from the air-water interface condition such that effects from discontinuity of the index of refraction at the surface disappear.

Azimuthal symmetry does not necessarily mean that the radiance has reached an asymptotic angular distribution, however. Obvious exceptions occur if the Sun is directly overhead or if the sea surface is illuminated through an optically thick cloud layer such that the radiance already is azimuthally symmetric before it enters the water.

As the depth increases in spatially uniform waters that contain no sources of radiance, apparent optical properties (AOPs) tend asymptotically to become inherent optical properties, as was illustrated, for example, by Mobley.¹ Recently Piening and McCormick² examined the tendency of four AOPs of azimuthally symmetric (or azimuthally integrated) radiance to approach their constant asymptotic values; specifically, they considered the diffuse attenuation coefficient, the irradiance reflectance, the radiance/irradiance ratio, and the mean cosine of the light field. The approach of these AOPs to their asymptotic shape is important because several methods for inferring absorption and scattering properties of ocean waters have been devised that give better results when these AOPs are nearly asymptotic.³⁻⁶

It is known that, if there is negligible azimuthal angle dependence, then the number of IOPs that can be inferred in an inverse problem analysis is greatly reduced.^{7,8} Also, if there is negligible azimuthal angle dependence, the computation time is dramatically reduced for any forward radiative transfer problem with a computer program (e.g., Hydrolight⁹) to determine the radiance.

In this paper we focus on the tendency of the radiance to approach its asymptotic polar and azimuthal angular shape. Section 2 contains an explanation of the tests that were done, and Section 3 contains the results of those tests.

The authors are with the Department of Mechanical Engineering, University of Washington, Seattle, Washington 98195-2600. A. Hakim's e-mail address is ahakim@u.washington.edu.

Received 2 November 2003; revised manuscript received 27 July 2004; accepted 19 August 2004.

0003-6935/04/315825-07\$15.00/0

© 2004 Optical Society of America

We consider the in-water radiative transfer equation¹

$$\begin{aligned} \mu \frac{\partial L(\tau, \mu, \varphi)}{\partial \tau} + L(\tau, \mu, \varphi) &= \varpi \int_0^{2\pi} d\varphi' \int_{-1}^1 \\ &\times d\mu' \tilde{\beta}(\mu', \varphi' \rightarrow \mu, \varphi) \\ &\times L(\tau, \mu', \varphi'), \\ \tau &\geq 0, \end{aligned} \quad (1)$$

where $L(\tau, \mu, \varphi)$ is the radiance at optical depth τ for polar angle $\theta = \cos^{-1} \mu$ with respect to τ and for azimuthal angle φ with $0 \leq \varphi \leq 2\pi$. The inherent optical properties ϖ and $\tilde{\beta}$ are the albedo of single scattering and the phase function, respectively. All quantities in Eq. (1) are implicitly a function of wavelength. The boundary conditions that we consider just above the surface for the radiance entering the water are for either a black sky ($i = 1$) or a diffuse illumination ($i = 2$):

$$L(0^-, \mu, \varphi) = F_i(\mu, \varphi), \quad 0 \leq \mu \leq 1, \quad i = 1, 2, \quad (2)$$

where

$$\begin{aligned} F_1(\mu, \varphi) &= E_d(0^-) \delta(\mu - \mu_{0,a}) \delta(\varphi - \varphi_0) / \mu_{0,a}, \\ 0 &\leq \mu_{0,a} \leq 1, \end{aligned} \quad (3)$$

$$F_2(\mu, \varphi) = \pi^{-1} E_d(0^-), \quad 0 \leq \mu \leq 1. \quad (4)$$

For both illumination conditions, $L(\tau \rightarrow \infty, \mu, \varphi) \rightarrow 0$. That is, the ocean is assumed to be very deep and to be illuminated by a solar beam with downward irradiance $E_d(0^-)$ just above the surface either in direction $(\mu_{0,a}, \varphi_0)$ or uniformly over all 2π incoming directions.

The first set of boundary conditions was selected to maximize the azimuthal dependence of the in-water radiance, whereas the second set with isotropic illumination was included to provide a comparison for the approach of the polar-angle-dependent radiance to its asymptotic shape.

One can best analyze the radiance for illumination condition 1 by separating it into two parts, one for the collided radiance and the other for the uncollided portion:

$$L(\tau, \mu, \varphi) = L_c(\tau, \mu, \varphi) + L_u(\tau, \mu, \varphi). \quad (5)$$

A Fourier expansion of the collided radiance gives¹⁰

$$L_c(\tau, \mu, \varphi) = \sum_{m=0}^M (2 - \delta_{m,0}) L_c^m(\tau, \mu) \cos[m(\varphi - \varphi_0)], \quad (6)$$

where the Fourier components of $L_c(\tau, \mu, \varphi)$ are

$$L_c^m(\tau, \mu) = (1/2\pi) \int_0^{2\pi} L_c(\tau, \mu, \varphi) \cos[m(\varphi - \varphi_0)] d\varphi, \quad (7)$$

with $\delta_{m,n} = 1$ for $m = n$ and $\delta_{m,n} = 0$ otherwise. Equation (6) makes it possible to replace the solution of the radiative transfer equation for $L(\tau, \mu, \varphi)$ by $(M + 1)$ independent radiative transfer equations for $L_c^m(\tau, \mu)$, $m = 0-M$ that depend on only τ and μ ,^{1,10-12} where $m = 0$ is the azimuthally symmetric equation. Each of these transfer equations has a corresponding set of eigenmodes for its respective eigenvalues.^{11,12} We denote the slowest spatially decaying eigenmode for each Fourier component, $L_c^m(\tau, \mu)$, by $\phi^m(\nu_1^m, \mu) \exp(-\tau/\nu_1^m)$. Radiance $L(\tau, \mu, \varphi)$ tends with increasing τ to become proportional to the eigenfunction $\phi^0(\nu_1^0, \mu)$, corresponding to the largest (i.e., asymptotic) eigenvalue ν_1^0 , where $\nu_1^0 > 1$ for $\varpi > 0$.^{6,11,12} [Another check on the eigenfunctions is that $\phi^m(\nu_1^m, \pm 1) = 0$ if $m \geq 1$, which is consistent with the requirement that the vertically upward and downward radiances be azimuthally symmetric.]

2. Approach to an Asymptotic Dependence on Azimuth

A. Azimuthal Angle Dependence

We examined with two different metrics the approach of the radiance to its azimuthally independent shape for increasing τ , i.e., $L(\tau, \mu, \varphi) \rightarrow L(\tau, \mu)$ for large τ . With the azimuthal average difference metric we used the ratio of the polar-angle average of the azimuthally integrated portion of the downward radiance to the polar-angle average of the downward radiance:

$$100 \max_{\varphi \in [0, 2\pi]} \left[1 - \frac{L_d(\tau)}{L_d(\tau, \varphi)} \right] \equiv \epsilon_{\varphi,a}(\tau), \quad (8)$$

where $\epsilon_{\varphi,a}(\tau)$ is the azimuthal average percent difference at depth τ and

$$L_d(\tau) = \int_0^1 L(\tau, \mu) d\mu, \quad (9)$$

$$L_d(\tau, \varphi) = \int_0^1 L(\tau, \mu, \varphi) d\mu. \quad (10)$$

For given values of μ_0 and of single-scattering albedo ϖ , we examined the values of $\epsilon_{\varphi,a}(\tau)$ versus τ for all φ , $0 \leq \varphi \leq 2\pi$. Even before performing any computations one can recognize that $L(\tau, \mu, \varphi)$ for the upward directions $-1 \leq \mu \leq 0$ naturally will be much more azimuthally symmetric than $L(\tau, \mu, \varphi)$ for the downward directions $0 \leq \mu \leq 1$, so we focus our attention primarily on the downward radiance, which explains the integration limits in Eqs. (9) and (10).

Similarly, we examined the dependence on depth of the maximum percent difference $\epsilon_{\varphi,m}(\tau)$, in values of the azimuthally dependent radiance with

$$100 \left[1 - \frac{\min_{\varphi \in [0, 2\pi]} L(\tau, \mu_0, \varphi)}{\max_{\varphi \in [0, 2\pi]} L(\tau, \mu_0, \varphi)} \right] \equiv \epsilon_{\varphi,m}(\tau), \quad (11)$$

the azimuthal maximum difference metric. Because of the dominance of small-angle scattering for ocean waters, the peak differences tend to occur for $\mu = \mu_0$, which are the values that we considered when we applied Eq. (11). In view of the incident illumination condition of Eq. (3) it is not surprising that the minimum values of L occur for $\varphi = \varphi_0 + \pi$ and the maximum values are at $\varphi = \varphi_0$ because no surface wind has been assumed.

B. Polar Angle Dependence

Because $L(\tau, \mu)$ becomes proportional to $\phi^0(v_1^0, \mu)\exp(-\tau/v_1^0)$ for large τ , we used the polar average difference metric, defined by

$$100 \max_{\mu \in [-1,1]} \left| 1 - \frac{\phi^0(v_1^0, \mu)/g_1^+(v_1^0)}{L(\tau, \mu)/E_d(\tau)} \right| \equiv \epsilon_{\mu,\alpha}(\tau), \quad (12)$$

where $\epsilon_{\mu,\alpha}(\tau)$ is the percent difference in polar average at depth τ and

$$g_1^+(v_1^0) = \int_0^1 \mu \phi^0(v_1^0, \mu) d\mu, \quad (13)$$

$$E_d(\tau) = \int_0^1 \mu L(\tau, \mu) d\mu. \quad (14)$$

For monodirectional illumination with given values of μ_0 and single-scattering albedo ϖ , we examined the values of $\epsilon_{\mu,\alpha}(\tau)$ versus τ for all μ , $-1 \leq \mu \leq 1$. We also used the criterion of Eq. (12) and examined the approach of the radiance to its asymptotic shape for the isotropic illumination given by Eq. (4).

3. Numerical Tests

The radiative transfer equation was solved by use of an analytic discrete-ordinates program written by Hakim following a procedure developed by Siewert.¹³ This discrete-ordinates program utilizes an expansion of collided radiance $L_c(\tau, \mu, \phi)$ in the formally exact functions that satisfy the radiative transfer equation.^{11,12} This has the advantage that the numerical discretization of μ is done on the explicit analytic form of the asymptotic eigenmode $\phi^0(v_1^0, \mu)$. To use this approach we extended Siewert's work to include refractive-index effects for the air-water interface by altering the discrete directions across the interface in the manner of Tanaka and Nakajima.¹⁴

The analytic discrete ordinates algorithm requires that the scattering phase function for scattering angle Θ (in radians) be expanded in a Legendre series, which we choose to denote as

$$\tilde{\beta}(\cos \Theta) = \sum_{n=0}^N \tilde{\beta}_n P_n(\cos \Theta), \quad (15)$$

where

$$\tilde{\beta}_n = (4\pi)^{-1}(2n+1)f_n, \quad (16)$$

so $\tilde{\beta}(\cos \Theta)$ is normalized by $f_0 = 1$. For the Henyey-Greenstein (HG) phase function,¹⁵ $f_n = f_1^n$, where f_1

is the mean cosine of the scattering phase function. But to compute the expansion coefficients $\tilde{\beta}_n$ for the Petzold phase function¹⁶ an analytical representation

$$\tilde{\beta}(\cos \Theta) = \exp\left(\sum_{n=0}^6 c_n \Theta^{n/2}\right) \quad (17)$$

proposed by Haltrin and Mankovsky¹⁷ for offshore-California waters was used, with their regression coefficients of $c_0 = 11.325$, $c_1 = -45.768$, $c_2 = 104.56$, $c_3 = -145.18$, $c_4 = 106.71$, $c_5 = -38.639$, and $c_6 = 5.5094$. Because of the highly forward-scattering nature of the phase functions, however, thousands of expansion coefficients may be needed for accurately computing of light fields. To make the problem computationally feasible we used the delta- L approximation in which the near-forward-scattering peak is stripped away by use of a delta function; i.e., the phase function is rewritten as

$$\tilde{\beta}(\cos \Theta) = 2\alpha\delta(1 - \cos \Theta) + (1 - \alpha)p(\cos \Theta), \quad (18)$$

where $0 \leq \alpha < 1$ is an optimally selected number and $p(\cos \Theta)$ is a phase function defined as in Eq. (15) but with a smaller number of expansion coefficients $\tilde{p}_n = (4\pi)^{-1}(2n+1)p_n$. Use of Eq. (18) in the radiative transfer equation does not change its form but introduces a scaling of the albedo and the optical depth to new albedo and depth values of ϖ' and τ' , respectively, for a radiative transfer equation with phase function $p(\cos \Theta)$:

$$\varpi' = \frac{\varpi(1 - \alpha)}{1 - \varpi\alpha}, \quad (19)$$

$$\tau' = \tau(1 - \varpi\alpha). \quad (20)$$

Use of the orthogonality relation for the Legendre polynomials shows that expansion coefficients f_n of $\tilde{\beta}(\cos \Theta)$ and coefficients p_n of $p(\cos \Theta)$ are related by

$$p_n = \frac{f_n - \alpha}{1 - \varpi\alpha}. \quad (21)$$

One way to compute the number α is to set $p_M = 0$, where M is suitably large. With this choice, which we used in our computations,

$$\alpha = f_M. \quad (22)$$

For example, setting $M = 1$ gives $\alpha = f_1$, which is the same as assuming that phase function $p(\cos \Theta)$ is isotropic.

Our analytic discrete coordinates program was benchmarked to within five significant figures against the results for the Haze- L and Cloud- C_1 problems obtained with two independent programs, one by Garcia and Siewert¹⁸ and the other by Siewert.¹³ The C_1 phase function, which is highly anisotropic, has 300 expansion coefficients, and we needed more than 400 discrete ordinates to accurately compute the radiance. The reason that we chose to use our own code is that we were unable to obtain the accuracy needed for radiances with the widely used Hydrolight

Table 1. First 260 Expansion Coefficients for the Petzold Offshore-California Phase Function for Use in Computing p_n from Eqs. (21) and (22)

n	f_{n+0}	f_{n+30}	f_{n+60}	f_{n+90}	f_{n+120}	f_{n+150}	f_{n+180}	f_{n+210}	f_{n+240}
0	1	0.3012	0.1970	0.1443	0.1119	0.0900	0.0743	0.0625	0.0534
1	0.8709	0.2960	0.1947	0.1430	0.1111	0.0894	0.0738	0.0622	0.0532
2	0.8146	0.2909	0.1925	0.1417	0.1102	0.0888	0.0734	0.0618	0.0529
3	0.7418	0.2861	0.1903	0.1404	0.1094	0.0882	0.0730	0.0615	0.0526
4	0.6886	0.2814	0.1881	0.1391	0.1085	0.0876	0.0725	0.0612	0.0524
5	0.6394	0.2768	0.1860	0.1379	0.1077	0.0871	0.0721	0.0608	0.0521
6	0.6010	0.2724	0.1840	0.1367	0.1069	0.0865	0.0717	0.0605	0.0519
7	0.5671	0.2682	0.1819	0.1355	0.1061	0.0859	0.0712	0.0602	0.0516
8	0.5395	0.2641	0.1800	0.1343	0.1053	0.0853	0.0708	0.0599	0.0514
9	0.5150	0.2601	0.1780	0.1331	0.1045	0.0848	0.0704	0.0596	0.0511
10	0.4942	0.2562	0.1761	0.1319	0.1037	0.0842	0.0700	0.0592	0.0509
11	0.4755	0.2524	0.1742	0.1308	0.1030	0.0837	0.0696	0.0589	0.0506
12	0.4591	0.2488	0.1724	0.1297	0.1022	0.0831	0.0692	0.0586	0.0504
13	0.4441	0.2452	0.1706	0.1286	0.1015	0.0826	0.0688	0.0583	0.0501
14	0.4307	0.2418	0.1688	0.1275	0.1007	0.0821	0.0684	0.0580	0.0499
15	0.4182	0.2384	0.1671	0.1264	0.1000	0.0816	0.0680	0.0577	0.0496
16	0.4068	0.2352	0.1654	0.1254	0.0993	0.0810	0.0676	0.0574	0.0494
17	0.3961	0.2320	0.1637	0.1243	0.0986	0.0805	0.0672	0.0571	0.0492
18	0.3862	0.2289	0.1621	0.1233	0.0979	0.0800	0.0669	0.0568	0.0489
19	0.3769	0.2259	0.1604	0.1223	0.0972	0.0795	0.0665	0.0565	0.0487
20	0.3681	0.2229	0.1588	0.1213	0.0965	0.0790	0.0661	0.0562	
21	0.3599	0.2200	0.1573	0.1203	0.0958	0.0785	0.0657	0.0559	
22	0.3521	0.2172	0.1557	0.1193	0.0951	0.0780	0.0654	0.0556	
23	0.3446	0.2145	0.1542	0.1183	0.0945	0.0775	0.0650	0.0554	
24	0.3376	0.2118	0.1527	0.1174	0.0938	0.0771	0.0646	0.0551	
25	0.3308	0.2092	0.1513	0.1164	0.0932	0.0766	0.0643	0.0548	
26	0.3244	0.2067	0.1498	0.1155	0.0925	0.0761	0.0639	0.0545	
27	0.3182	0.2042	0.1484	0.1146	0.0919	0.0757	0.0636	0.0542	
28	0.3123	0.2017	0.1470	0.1137	0.0913	0.0752	0.0632	0.0540	
29	0.3067	0.1993	0.1457	0.1128	0.0906	0.0747	0.0629	0.0537	

program.⁹ Inconsistencies between asymptotic results obtained from Hydrolight and a traditional discrete ordinate program¹⁹ were identified earlier.²⁰ Subsequently, large errors in values of radiances from Hydrolight were observed by Chalhoub *et al.*²¹ even though errors in the scalar and planar irradiances were not large.

For the asymptotic radiance tests here, both the HG and the Petzold offshore-California phase functions were used. The latter describes the scattering phase function for typical case 1 waters, for example. The HG phase function was selected to give the same asymmetry factor, $f_1 = 0.870905$, as the Petzold phase function. For the computations performed, we set $M = 250$. No changes in the computed radiances were observed when M was increased beyond this value. The results for the f_n coefficients are given in Table 1 for the Petzold offshore-California phase function and are also available at http://faculty.washington.edu/mccor/ocean_optic_index.html.

Although the radiance at large optical depths becomes proportional to $\phi^0(\nu_1^0, \mu)\exp(-\tau/\nu_1^0)$, the rate at which the radiance approaches this shape depends on the separation of the largest few eigenvalues of the $m = 0$ component. These eigenvalues in turn depend on single-scattering albedo ω and on the phase function. Figure 1 shows the largest three eigenvalues of the $m = 0$ component of the transfer equation as a function of ω for the Petzold offshore-California

phase function. These eigenvalues were computed with reduced phase function p and were transformed back by use of the relation $\nu = \nu'/(1 - \omega\alpha)$. Not shown is the behavior as $\omega \rightarrow 1$, for which $\nu_1^0 \rightarrow \infty$, $\nu_2^0 \rightarrow 3.13596$, and $\nu_3^0 \rightarrow 2.12843$. From Fig. 1 it is

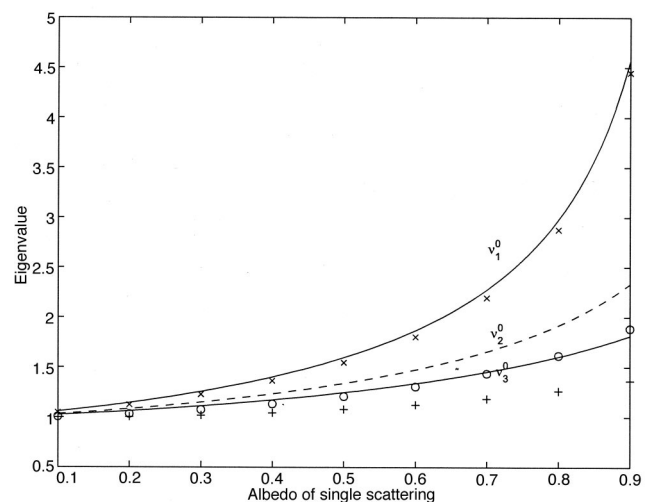


Fig. 1. Largest three eigenvalues for the $m = 0$ mode of the transfer equation as a function of the albedo of single scattering for the Petzold phase function (continuous curves). Selected results for the HG phase function are also shown: crosses, ν_1^0 ; open circles, ν_2^0 ; pluses, ν_3^0 .

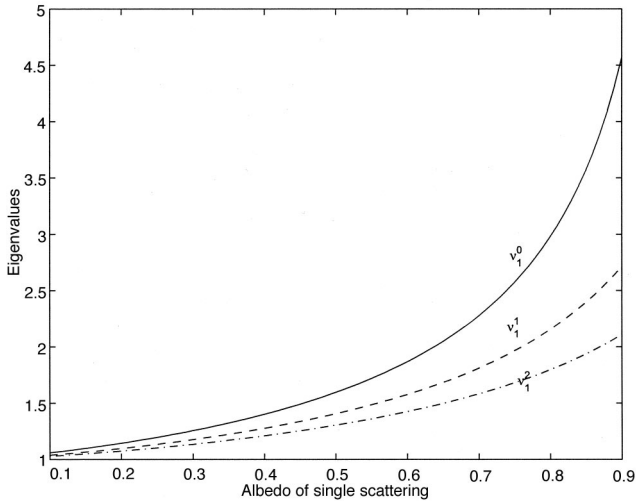


Fig. 2. Largest eigenvalues for the $m = 0, 1, 2$ modes of the transfer equation as a function of the albedo of single scattering for the Petzold phase function.

clear that these eigenvalues are close together for $\varpi \leq 0.3$ and are approximately equal to unity. The implication of this near degeneracy of eigenvalues means that several eigenmodes can contribute to the radiance for small ϖ values and that the uncollided radiance can become nonnegligible. The light field tends to be nearly unmeasurable at those depths where the radiance tends to become asymptotic, however. For this reason the subsequent simulations that we performed were for two values of the single-scattering albedo, $\varpi = 0.5$ and $\varpi = 0.9$, that span the range of values that are usually encountered in ocean waters.

The simulations for the metrics of Eqs. (8), (11), and (12) were performed with three values of solar beam incident polar angle: $\theta = 30^\circ, 45^\circ, 60^\circ$. An index of refraction of $n = 1.34$ was used for the air-water interface, but the asymptotic results reported here are virtually the same as those for which Fresnel reflection and refraction effects have not been accounted for because of the large optical depths where the asymptotic distribution is approached.

Figure 1 also shows that the largest eigenvalue of the azimuthally symmetric transfer equation ($m = 0$) for the selected HG phase function is nearly equal to that for the Petzold phase function. However, the two next higher eigenvalues are considerably smaller than the corresponding eigenvalues for the Petzold phase function; hence the HG eigenmodes decrease more rapidly with depth. This result indicates that the light field calculated with the HG phase function will achieve its asymptotic values faster, a result that we confirmed in subsequent computations.

Figure 2 shows the largest eigenvalues v_1^m for the $m = 0, 1, 2$ components of the transfer equation as a function of albedo of single scattering. These values indicate that every azimuthally dependent eigenmode of the radiance that is caused by the surface incident illumination will persist to large depths.

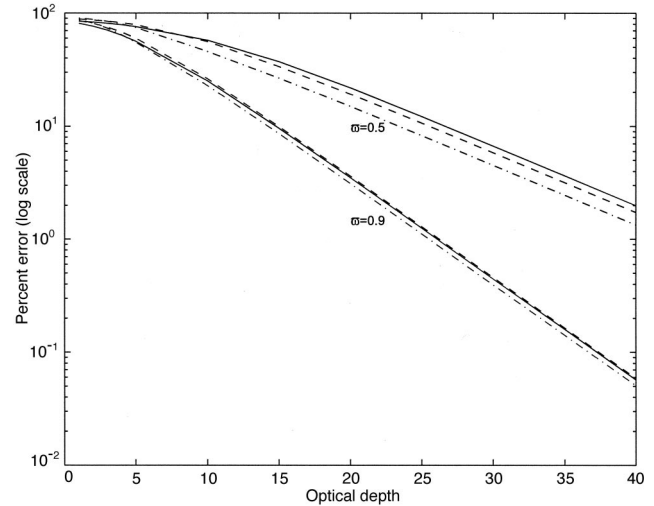


Fig. 3. Azimuthal average percent difference metric of Eq. (8) as a function of optical depth for the HG phase function. Results with incident beam angle $\theta = 60^\circ$, solid curves; $\theta = 45^\circ$, dashed curves; $\theta = 30^\circ$, dashed-dotted curves.

A. Azimuthal Angle Dependence

Figure 3 shows the average difference metric of Eq. (8) for the HG phase function as a function of optical depth for selected incident beam angles and albedoes of single scattering. The figure shows a trend that is common to all the results obtained: For $\varpi = 0.9$ the radiance approaches its asymptotic value faster than for $\varpi = 0.5$. This is so because the separation between v_1^0 and v_1^1 is greater for larger ϖ , as shown in Fig. 2. It is also clear that for $\varpi = 0.9$ the radiance is azimuthally symmetric to within 1% for $\tau > 25$, whereas for $\varpi = 0.5$ this occurs for $\tau > 40$. These results do not depend strongly on the incident beam angle.

Figure 4 illustrates the azimuthal maximum difference metric of Eq. (11) as a function of optical

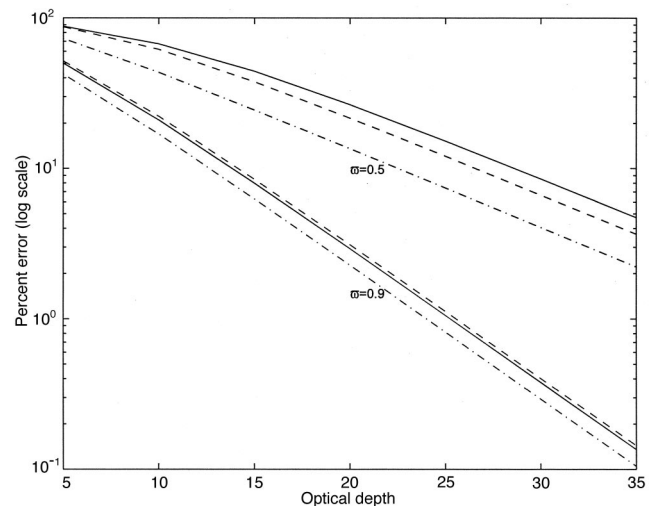


Fig. 4. Same as Fig. 3 but for the azimuthal maximum percent difference metric of Eq. (11).

Table 2. Azimuthal Average Percent Difference Metric of Eq. (8) for Selected Optical Depths for the Petzold Phase Function with Incident Beam Directions of 30°, 45°, and 60°

τ	$\varpi = 0.5$			$\varpi = 0.9$		
	30°	45°	60°	30°	45°	60°
5	90.8	91.4	87.1	77.3	78.1	71.3
10	79.9	75.7	25.9	44.9	44.6	36.4
20	44.5	35.3	11.3	11.0	10.7	17.7
30	19.8	15.4	7.4	2.5	2.3	1.9
40	8.5	6.6	4.8	0.5	0.5	0.4

Table 3. Polar Average Percent Difference Metric of Eq. (12) for Selected Optical Depths for the Petzold Phase Function with Incident Beam Directions of 30°, 45°, and 60°

τ	$\varpi = 0.5$			$\varpi = 0.9$		
	30°	45°	60°	30°	45°	60°
15	40.2	35.6	32.2	3.5	3.0	6.2
20	12.9	10.5	8.5	1.3	0.9	1.5
30	5.2	5.1	3.4	0.5	0.2	0.8
40	2.2	1.2	1.1	0.01	0.06	0.1

depth. For $\varpi = 0.9$ and for all incident beam angles that we considered, the radiance is also azimuthally symmetric to within $\sim 1\%$ for $\tau > 25$ for the maximum difference metric. The results in Figs. 3 and 4 are quite similar, except that in Fig. 4 the maximum difference metric shows a greater dependence on the illumination angle.

Table 2 shows the results for the azimuthal average difference metric for the Petzold offshore-California phase function. Comparison of these results with those obtained with the HG phase function in Fig. 3 shows that the light field calculated by use of the Petzold phase function becomes azimuthally symmetric at larger optical depths.

B. Polar Angle Dependence

Figure 5 shows the average percent difference metric of Eq. (12) for the HG phase function as a function of optical depth. It can be seen that, except for $\varpi = 0.9$ and $\theta = 60^\circ$, the radiance approaches its asymptotic polar angle dependence faster for diffuse illumination than for beam illumination. Furthermore, comparison of these results with those obtained from the two azimuthal difference metrics shows that the radiance

approaches its asymptotic polar-angle dependence much faster than it approaches its azimuthally symmetric shape, even though each scattering event is symmetric in the local azimuthal direction about a photon's precollision direction. This is so because of the persistence of the asymptotic eigenmodes for the azimuthal components that are excited with monodirectional surface illumination, as shown in Fig. 2. Table 3 lists the results with this metric for the Petzold phase function.

4. Comments

The nonasymptotic dependence of the radiance will become more important for applied ocean optics applications after radiance measurements become routinely made. At present, with typical detectors that measure only a scalar irradiance, a planar irradiance, or the vertically upward radiance, the azimuthal dependence of the radiance is lost. Thus it is sufficient to know just the asymptotic approach of integral quantities such as the irradiance ratio that were studied previously,² because they approach their asymptotic shapes much more rapidly than does the radiance.

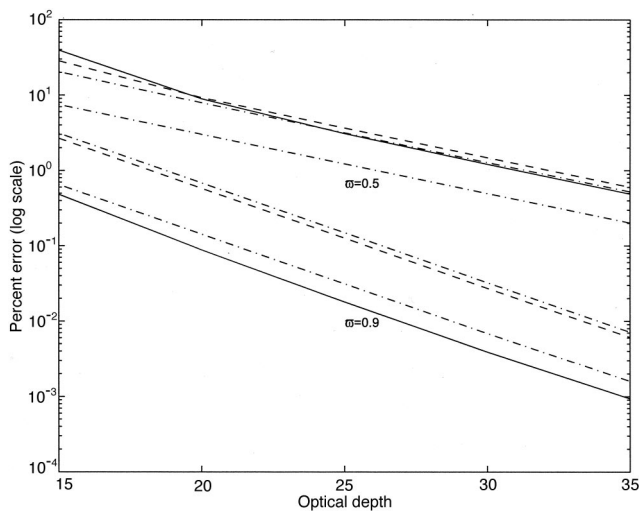


Fig. 5. Polar average percent difference metric of Eq. (12) as a function of optical depth for the HG phase function. Results with incident beam angle $\theta = 60^\circ$, solid curves; $\theta = 45^\circ$, dashed curves; $\theta = 30^\circ$, dashed-dotted curves.

Appendix A. Air-Water Interface Condition

The ocean surface was assumed to be flat (i.e., no wind), and wave focusing effects were ignored²² to allow the illumination beneath the surface to be treated with classic Fresnel transmission and reflection techniques. The air-water interface condition beneath the surface is

$$\begin{aligned}
 L(0^+, \mu, \varphi) &= \int_0^{2\pi} d\varphi' \int_0^1 d\mu' L(0^+, -\mu', \varphi') \\
 &\times R_{ww}(\mu, \mu', \varphi, \varphi') + \int_0^{2\pi} d\varphi' \\
 &\times \int_0^1 d\mu' L(0^-, \mu', \varphi') \\
 &\times T_{aw}(\mu, \mu', \varphi, \varphi'), \quad 0 \leq \mu \leq 1,
 \end{aligned} \tag{A1}$$

where, for a flat surface,^{1,14,23}

$$R_{ww}(\mu, \mu', \varphi, \varphi') = r_{ww}(\mu)\delta(\mu - \mu')\delta(\varphi - \varphi'),$$

$$\mu \geq (1 - 1/n^2)^{1/2}, \quad (\text{A2})$$

$$= \delta(\mu - \mu')\delta(\varphi - \varphi'),$$

$$\mu < (1 - 1/n^2)^{1/2}, \quad (\text{A3})$$

$$T_{aw}(\mu, \mu', \varphi, \varphi') = n^2 t_{aw}(g(\mu))\delta(g(\mu) - \mu')\delta(\varphi - \varphi'), \quad (\text{A4})$$

with

$$r_{ww}(\mu) = \frac{1}{2} \left\{ \left[\frac{\mu - ng(\mu)}{\mu + ng(\mu)} \right]^2 + \left[\frac{n\mu - g(\mu)}{n\mu + g(\mu)} \right]^2 \right\}, \quad (\text{A5})$$

$$t_{aw}(\mu) = 2n\mu f(\mu) \left\{ \left[\frac{1}{\mu + nf(\mu)} \right]^2 + \left[\frac{1}{n\mu + f(\mu)} \right]^2 \right\}, \quad (\text{A6})$$

$$f(\mu) = [1 - (1 - \mu^2)/n^2]^{1/2}, \quad (\text{A7})$$

$$g(\mu) = [1 - n^2(1 - \mu^2)]^{1/2}. \quad (\text{A8})$$

B. D. Piening was supported by the Mary Gates Endowment for Students undergraduate research program at the University of Washington. Early discussions with Todd Bowers were helpful, as were comments from the reviewers.

References

1. C. D. Mobley, *Light and Water Radiative Transfer in Natural Waters* (Academic, New York, 1994), Secs. 4.2, 5.7, and 9.6.
2. B. D. Piening and N. J. McCormick, "Asymptotic optical depths in source-free ocean waters," *Appl. Opt.* **42**, 5382–5387 (2003).
3. R. A. Leathers and N. J. McCormick, "Ocean inherent optical property estimation from irradiances," *Appl. Opt.* **36**, 8685–8698 (1997).
4. L. K. Sundman, R. Sanchez, and N. J. McCormick, "Ocean optical source estimation with widely spaced irradiance measurements," *Appl. Opt.* **37**, 3793–3803 (1998).
5. R. A. Leathers and N. J. McCormick, "Algorithms for ocean-bottom albedo determination from in-water natural-light measurements," *Appl. Opt.* **38**, 3199–3205 (1999).
6. R. A. Leathers, C. S. Roesler, and N. J. McCormick, "Ocean inherent optical property determination from in-water light field measurements," *Appl. Opt.* **38**, 5096–5103 (1999).
7. N. J. McCormick, "Transport scattering coefficients from reflection and transmission measurements," *J. Math. Phys.* **20**, 1504–1507 (1979).
8. A. H. Hakim and N. J. McCormick, "Ocean optics estimation for absorption, backscattering, and phase function parameters," *Appl. Opt.* **42**, 931–938 (2003).
9. C. D. Mobley and L. K. Sundman, *Hydrolight 4.1* (Sequoia Scientific, Redmond, Wash., 2000).
10. S. Chandrasekhar, *Radiative Transfer* (Dover, New York, 1960), Sec. 48.
11. I. Kuščer and N. J. McCormick, "Some analytical results for radiative transfer in thick atmospheres," *Transp. Theory Stat. Phys.* **20**, 351–381 (1991).
12. G. W. Kattawar, ed., *Selected Papers on Multiple Scattering in Plane Parallel Atmospheres and Oceans: Methods*, Vol. MS42 of SPIE Milestone Series (SPIE, Bellingham, Wash., 1991).
13. C. E. Siewert, "A concise and accurate solution to Chandrasekhar's basic problem in radiative transfer," *J. Quant. Spectrosc. Radiat. Transfer* **64**, 109–130 (2000).
14. M. Tanaka and T. Nakajima, "Effects of oceanic turbidity and index of refraction of hydrosols on the flux of solar radiation in the atmosphere-ocean system," *J. Quant. Spectrosc. Radiat. Transfer* **18**, 93–111 (1977).
15. L. C. Henyey and J. L. Greenstein, "Diffuse radiation in the galaxy," *Astrophys. J.* **93**, 70–83 (1941).
16. T. J. Petzold, "Volume scattering functions for selected ocean waters," SIO Ref. 71–78 (Scripps Institution of Oceanography, La Jolla, Calif., 1972).
17. V. I. Haltrin and V. I. Mankovsky, "Analytical representation of experimental light scattering phase functions measure in seas, oceans and Lake Baykal," proceedings of the 2002 IEEE International Geoscience and Remote Sensing Symposium, 24–28 June 2002, Toronto, Canada, available on CD ROM from the Geoscience and Remote Sensing Society, <http://www.ewh.ieee.org/soc/grss/igarss.html>.
18. R. D. M. Garcia and C. E. Siewert, "Benchmark results in radiative transfer," *Transp. Theory Stat. Phys.* **14**, 437–483 (1985).
19. Z. Jin and K. Stamnes, "Radiative transfer in nonuniformly refracting layered media: atmosphere-ocean system," *Appl. Opt.* **33**, 431–442 (1994).
20. C. D. Mobley, B. Gentili, H. R. Gordon, Z. Jin, G. W. Kattawar, A. Morel, P. Reinertman, K. Stamnes, and R. H. Stavn, "Comparison of numerical models for computing underwater light fields," *Appl. Opt.* **32**, 7484–7504 (1994).
21. E. S. Chalhoub, H. F. Campos Velho, R. D. M. Garcia, and M. T. Vilhena, "A comparison of radiances generated by selected methods of solving the radiative-transfer equation," *Transp. Theory Stat. Phys.* **32**, 473–503 (2003).
22. J. R. V. Zaneveld, E. Boss, and A. Barnard, "Influence of surface waves on measured and modeled irradiance profiles," *Appl. Opt.* **40**, 1442–1449 (2001).
23. G. E. Thomas and K. Stamnes, *Radiative Transfer in the Atmosphere and Ocean* (Cambridge U. Press, Cambridge, UK, 1999), App. E.